Chapter 17
Solitary Wave Collisions

Sergey V. Dmitriev and Dimitri J. Frantzeskakis

17.1 Introduction and Setup

The well-known (see, e.g., [1] and references therein) elastic nature of the interaction among solitons in the completely integrable one-dimensional (1D) nonlinear Schrödinger (NLS) equation or in the completely integrable *Ablowitz–Ladik* (AL) lattice [2, 3] generally ceases to exist when perturbations come into play. This is due to the fact that, generally, perturbations are destroying the complete integrability and as a result many different effects in soliton interactions come into play. More specifically, in perturbed continuous (or discrete) NLS equations the outcome of the the collision process (i.e., the soliton trajectories and soliton characteristics) depends on the phase difference between two colliding solitons, emission of continuum radiation during soliton collisions, as well as the excitation of solitons' internal modes.

Here, we will discuss soliton collisions in the discrete NLS equation in the usual form,

$$i\dot{u}_n = -C\Delta_2 u_n - |u_n|^2 u_n. \tag{17.1}$$

We will firstly discuss the case of *weak discreteness*, $C \gg 1$, which is a nearly integrable case: in the limit $C \to \infty$, Eq. (17.1) becomes the integrable 1D continuous NLS equation $i\partial_t u = -(1/2)\partial_x^2 u - |u|^2 u$, while the effect of a weak discreteness may be partially accounted for by the perturbation term proportional to $\partial_x^4 u$. The effect of such a weak discreteness on soliton collisions has been studied in Refs. [4, 5]. Then the case of *strong discreteness*, $C \sim 1$, will be discussed following the results reported in [6] for Eq. (17.1), and also the results reported in [7] for the following model:

$$i\dot{u}_n = -C\Delta_2 u_n - \delta|u_n|^2 u_n - \frac{1-\delta}{2}|u_n|^2(u_{n+1}+u_{n-1}) + \varepsilon|u_n|^4 u_n, \tag{17.2}$$

S.V. Dmitriev (✉)
Institute for Metals Superplasticity Problems RAS, 450001 Ufa, Khalturina 39, Russia
e-mail: dmitriev.sergey.v@gmail.com

P.G. Kevrekidis, *The Discrete Nonlinear Schrödinger Equation*, STMP 232,
311–327, DOI 10.1007/978-3-540-89199-4_17,

where δ, ε are two different perturbation parameters, providing tunable degree of nonintegrability. In particular, for $\delta = \varepsilon = 0$, Eq. (17.2) is reduced to the AL lattice [2, 3], which is integrable even in the case of strong discreteness. On the other hand, for $\varepsilon = 0$, Eq. (17.2) is reduced to the so-called *Salerno model* [8]. For $\varepsilon = 0$ and $\delta = 1$, Eq. (17.2) reduces to Eq. (17.1). Equation (17.2) has two integrals of motion, namely it conserves a modified norm and energy (Hamiltonian) [7]. For $\delta = \varepsilon = 0$ it supports the exact AL soliton solution [2, 3]

$$u_n(t) = \sqrt{2C}\sinh\mu\frac{\exp[ik(n-x)+i\alpha]}{\cosh[\mu(n-x)]}\,, \quad x = x_0 + \frac{2Ct}{\mu}\sinh\mu\sin k\,,$$
$$\alpha = \alpha_0 + 2Ct\left[\cos k\cosh\mu + \frac{k}{\mu}\sinh\mu\sin k - 1\right], \tag{17.3}$$

where the parameters x_0 and α_0 are the initial coordinate and phase of the soliton, respectively, while the soliton's inverse width μ and the parameter k define the soliton's amplitude A and velocity V through the equations:

$$A = \sqrt{2C}\sinh\mu\,, \quad V = \frac{\sqrt{2C}}{\mu}\sinh\mu\sin k\,. \tag{17.4}$$

Finally, we review the results reported in the literature for the collisions of solitons in some physically relevant settings where discrete NLS equations are key models. These settings include optical waveguide arrays (in the optics context), and Bose–Einstein condensates (BECs) confined in optical lattices (in the atomic physics context).

17.2 Collisions in the Weakly Discrete NLS Equation

Examples of two-soliton collisions in the weakly discrete Eq. (17.1) (for $C = 15$) are presented in Fig. 17.1. Initial conditions were set employing the exact two-soliton solution to the integrable NLS equation [9, 10]. The out-of-phase collision in (a) and the in-phase collision in (b) are practically elastic, but they are very different in the sense that in (a) solitons repel each other and their cores do not merge at the collision point while in (b) the situation is opposite. The collision in (b) corresponds to the separatrix two-soliton solution to the integrable NLS equation [5]. Near-separatrix (nearly in-phase) collisions are strongly inelastic, as exemplified in (c), where the solitons emerge from the collision with different amplitudes and velocities. In (d), solitons' amplitudes after collision, $\tilde{A}_i$, are presented as the functions of the initial phase difference $\Delta\alpha_0$. Note the extreme sensitivity of the collision outcome to the initial phase difference $\Delta\alpha_0$ for the near-separatrix collisions ($\Delta\alpha_0 \approx 0$). Of particular importance is the fact that in the inelastic near-separatrix collisions in the regime of weak discreteness the energy given to the soliton's internal modes and to the radiation is negligible in comparison to the energy exchange between the

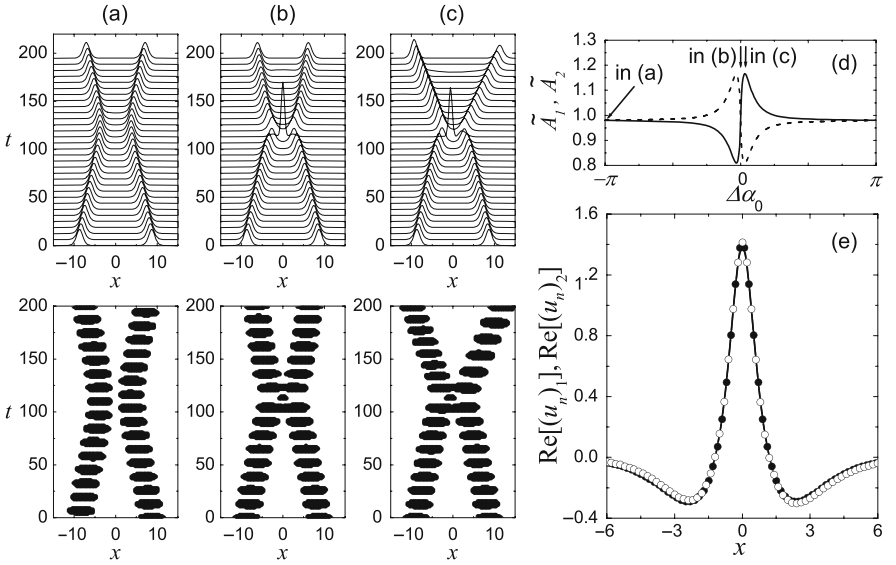

Fig. 17.1 Collisions in the weakly discrete NLS equation Eq. (17.1) at $C = 15$. *Upper panels* in (**a**)–(**c**) show $|u(x,t)|^2$, while *bottom panels* show the regions with $\mathrm{Re}[u(x,t)] > 0.3$ in order to reveal the difference in the relative initial phase $\Delta\alpha_0$ of solitons: in (**a**), (**b**), and (**c**), $\Delta\alpha_0 = -\pi,\ 0,$ and 0.1, respectively. (**d**) Soliton amplitudes after collision $\tilde{A}_i$ as functions of $\Delta\alpha_0$. The parameters of the solitons before the collision are $A_1 = A_2 = 0.98$, $V_1 = -V_2 = 0.05$. (**e**) Comparison of the real parts for two different exact two-soliton solutions to the NLS equation at the collision point. Imaginary parts are similarly close. The first solution (*dots*) has $A_1 = A_2 = 1$, $V_1 = -V_2 = 0.01$, while the second one (*circles*) has $A_1 = 1.1$, $A_2 = 0.9$, $V_1 = 0.0909$, $V_2 = -0.1111$. These two solutions have the same norm and momentum and $\Delta\alpha_0 = 0$. (After Ref. [5]; © 2002 APS.)

solitons [4]. This is the main feature of the so-called radiationless energy exchange (REE) effect in soliton collisions [11]. The REE in near-separatrix collisions can be understood by the fact that the profiles of two different two-soliton solutions to integrable NLS equation can be very close to each other at the collision point. An example is given in (e) by comparing the real parts of solutions with $A_1 = A_2 = 1$, $V_1 = -V_2 = 0.01$ (dots) and $A_1 = 1.1$, $A_2 = 0.9$, $V_1 = 0.0909$, $V_2 = -0.1111$ (circles). These two solutions have the same norm and momentum and $\Delta\alpha_0 = 0$. Their imaginary parts are similarly close. The presence of even weak perturbation can easily transform such close solutions one into another without violation of the conservation laws remaining in the weakly perturbed system.

For sufficiently small collision velocity, the REE effect can result in the fractal soliton scattering in the weakly discrete NLS equation [4, 5]. Fractal soliton scattering in the weakly perturbed NLS equation was explained qualitatively in the frame of a very simple model [4] and for the generalized NLS equation in the context of a more elaborate collective variable approach [12, 13], based on the method of Karpman and Solov'ev [14].

In Fig. 17.2a the solitons' velocities after collision, $\tilde{V}_i$, are shown as functions of the initial phase difference $\Delta\alpha_0$ for Eq. (17.1) at $C = 25$. Initial velocities and

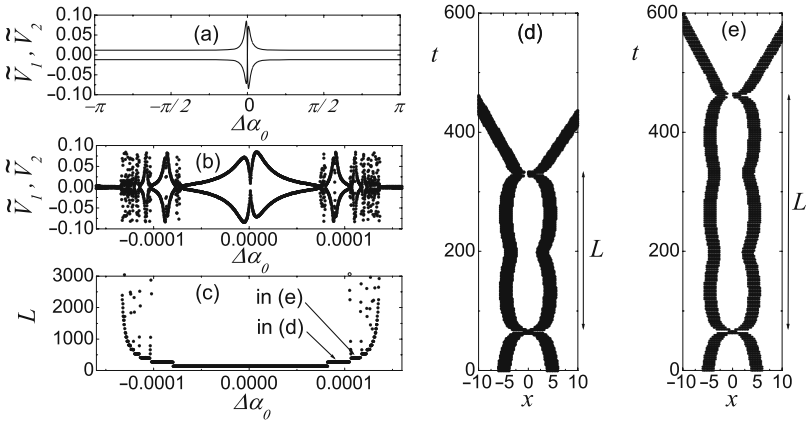

Fig. 17.2 Fractal soliton scattering in the weakly discrete NLS equation (17.1) at $C = 25$. (**a**) Soliton velocities after collision, $\tilde{V}_i$, as functions of initial phase difference $\Delta\alpha_0$. (**b**) Blowup of the region in (a) in the vicinity of $\Delta\alpha_0 = 0$. (**c**) Lifetime of the two-soliton bound states as function of $\Delta\alpha_0$. (**d**), (**e**) Examples of two-soliton bound states with different lifetime L. Regions of the x, t plane with $|u_n|^2 > 0.3$ are shown. The corresponding values of the initial phase difference $\Delta\alpha_0$ are indicated in (c). Initial soliton velocities are $V_1 = -V_2 = 0.012$ and initial amplitudes are $A_1 = A_2 = 1$

amplitudes are $V_1 = -V_2 = 0.012$ and $A_1 = A_2 = 1$, respectively. The collisions are inelastic in the vicinity of $\Delta\alpha_0 = 0$ where the solitons' velocities after collision differ considerably from their initial velocities. Blowup of the narrow region in the vicinity of $\Delta\alpha_0 = 0$ presented in (b) reveals a complex behavior of $\tilde{V}_i(\Delta\alpha_0)$. Smooth regions of these functions are separated by apparently chaotic regions. However, any chaotic region being expanded reveals the property of self-similarity at different scales (not shown in Fig. 17.2 but can be found in [4, 5]). The fractal soliton scattering can be explained through the following two facts: (i) in a weakly discrete system, the solitons attract each other with a weak force and (ii) the REE between colliding solitons is possible. As it is clearly seen from Fig. 17.2b, the chaotic regions appear where $\tilde{V}_i$ in smooth regions become zero. In these regions, the solitons after collision gain very small velocities so that they cannot overcome their mutual attraction and collide again. In the second collision, due to the momentum exchange, the solitons can acquire an amount of energy sufficient to escape each other, but there exists a finite probability to gain the energy below the escape limit. In the latter case, the solitons will collide for a third time, and so on. Physically, the multiple collisions of solitons can be regarded as the two-soliton bound state with certain lifetime L (two examples are given in Fig. 17.2d, e). The probability P of the bound state with the lifetime L was estimated to be $P \sim L^{-3}$ and this rate of decreasing of P with increase in L does not depend on the parameters of the colliding solitons [4].

Importantly, the REE effect in near-separatrix collisions has been predicted from the analysis of the two-soliton solution to the *unperturbed* integrable NLS equation [5] and thus, the precise form of the perturbation is not really important for the appearance of this effect. Moreover, it has been demonstrated that in the systems

with more than one perturbation term, the collisions can be nearly elastic even in the vicinity of $\Delta\alpha_0 = 0$ when the effects of different perturbations cancel each other [5, 7].

17.3 Collisions in the Strongly Discrete NLS Equation

Let us now consider the strongly discrete NLS Eq. (17.1) with the coupling constant C now assumed to be a parameter of order $O(1)$. In such a case, soliton collisions may in principle be studied by means of a variational approximation (VA), as the ones used in various works (see, e.g., [15, 16]) to study discrete soliton solutions of the discrete nonlinear Schrödinger (DNLS) equation. However, in the case of soliton collisions under consideration, a direct application of VA may produce equations for the soliton parameters that could be very difficult to be expressed in an explicit form and, thus, to be treated analytically or numerically. A simple variant of VA was adopted in [6], where the variational ansatz was considered to be a combination of two *discrete spikes*, which was subsequently substituted into the *continuous* NLS equation, with the Lagrangian $\int_{-\infty}^{+\infty}\left[i\left(u^*\dot{u}-u\dot{u}^*\right)-|u_x|^2+|u|^4\right]dx$. Using this discreteness motivated ansatz in the continuum Lagrangian of the model, the resulting variational equations predicted that the collision of two solitons with large velocities leads to bounce, while the collision with small velocities gives rise to *merger* of the solitons.

The above result can be confirmed by means of systematic simulations. Here, following the analysis of [6], we use an initial condition for the DNLS equation (17.1) suggested by the AL model (see Eq. (17.3)), namely,

$$u_0 = B\,\mathrm{sech}\left[W^{-1}(n-x_1)\right]\exp\left[ia(n-x_1)+\left(\frac{i}{2}\right)\Delta\phi\right] + B\,\mathrm{sech}\left[W^{-1}(n-x_2)\right]\exp\left[-ia(n-x_2)-\left(\frac{i}{2}\right)\Delta\phi\right]. \quad (17.5)$$

It is clear that Eq. (17.5) is a superposition of two far separated pulses with common amplitude B and width W, initial phase difference $\Delta\phi$, and initial positions at $x_{1,2}$. The parameter a denotes the soliton wave number and, in fact, determines the initial soliton speed. Fixing the soliton width as, e.g., $W = 1$, and using a as a main control parameter, it is possible to study outcomes of the collision for several different values of the amplitude B, including $B = \sinh(1/W) \approx 1.1752$ (corresponding to the AL soliton), $B = 1$ (corresponding to the continuum NLS limit), and another smaller value, $B = 1/\sinh(1/W) \approx 0.851$. Although these values are not very different, the results obtained for them may differ dramatically, and they adequately represent the possible outcomes of the collision. Moreover, using the initial condition Eq. (17.5), it is also possible to study on-site (OS) and inter-site (IS) collisions (with the central point located, respectively, OS or at a midpoint between sites), varying the initial positions x_1 and x_2.

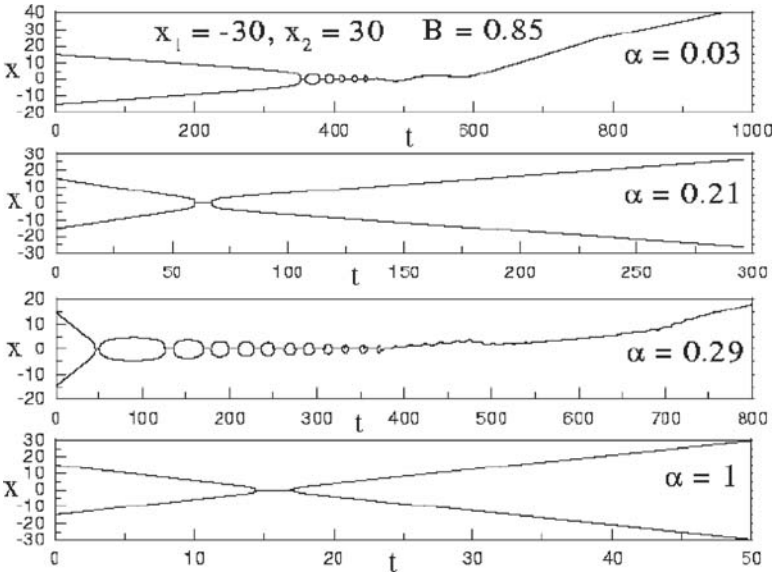

Fig. 17.3 The on-site collision, with $x_{1,2} = \pm 30$, for various values of the parameter a in the case of $B = 0.851$. The intervals of merger with spontaneous symmetry breaking are separated by regions of quasi-elastic collisions. In all the cases displayed herein $C = 0.5$

Figure 17.3 depicts several collision and merger scenarios that we now explain in some detail. Let us first consider the case of OS collisions, with $x_{1,2} = \pm 30$, and initial soliton amplitude $B = 1.175$ and 1 (below we will also consider that the solitons have the same phase, i.e., $\Delta\phi = 0$). In the former case ($B = 1.175$), the solitons cannot collide for $a < 0.550$ (as in this case these "taller" solitons encounter a higher Peierls–Nabarro [PN] barrier), they move freely and collide merging to a single pulse for $0.550 < a < 2.175$ (with multiple collisions, if a is close to the upper border of this interval), and they collide quasi-elastically for $a > 2.175$. In the latter case ($B = 1$), and for $0 < a < 0.7755$, the colliding solitons merge into a single pulse, while for $a > 0.7756$, the solitons undergo a quasi-elastic collision (as they separate after the collision). It is worth noting that these basic features of this phenomenology (for $B = 1$) are correctly predicted by the aforementioned VA devised in [6]. Nevertheless, some more peculiar characteristics can also be identified, since in the interval $0 < a < 0.7755$, there exist two subintervals, namely $0 < a < 0.711$, where the solitons fuse into one after a single collision, and $0.711 < a < 0.7755$, where the fusion takes place after multiple collisions. Finally, in the case of the smaller initial amplitude, $B = 0.851$, a new feature is found in intervals $a < 0.203$ and $0.281 < a < 0.3$. There, the solitons merge after multiple collisions, which is accompanied by strong *symmetry breaking* (SB): the resulting pulse moves to the left or to the right, at a well-defined value of the velocity, as is shown in Fig. 17.4. Between these intervals, i.e., at $0.203 < a < 0.281$, as well as in the case $a > 0.3$, the collisions are quasi-elastic.

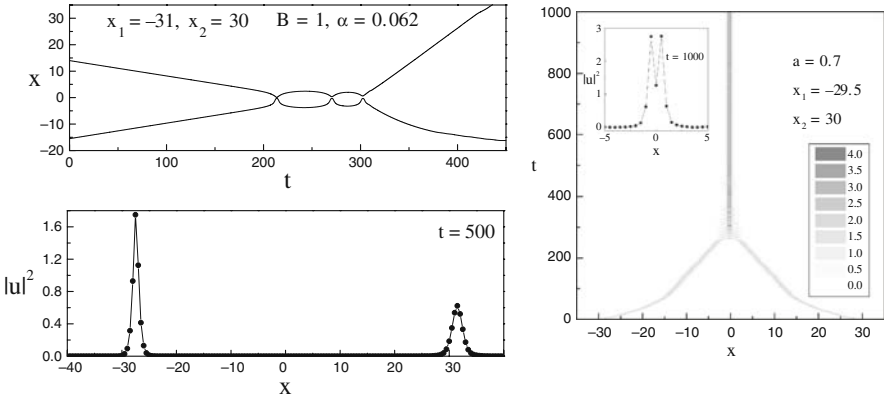

Fig. 17.4 *Left panel*: The inter-site collision, with $x_1 = -31$, $x_2 = 30$, for $a = 0.062$ and $B = 1$. Both trajectories of the colliding solitons (*top*) and their eventual profiles in terms of $|u|^2 \equiv |u_n|^2$ (*bottom*) are shown, with the latter picture illustrating the symmetry breaking. *Right panel*: The quarter-site collision ($x_1 = -29.5$, $x_2 = 30$) for $a = 0.7$ and $B = 1.175$. Shown are the soliton trajectories and the formation of an "M"-shaped merger (see inset). In all the cases displayed herein $C = 0.5$

It should be noted that the SB mechanism and the collision-induced momentum generation (recall that the lattice momentum is not conserved) were analyzed in [6]. As discussed in that work, the SB may be deterministic or spontaneous. The former one is accounted for by the location of the collision point relative to the lattice, and/or the phase shift between the solitons, while the momentum generated during the collision due to the phase shift was found to depend on the solitons' velocities. As far as spontaneous SB is concerned, the modulational instability of a quasi-flat plateau temporarily formed in the course of the collision was suggested as a possible explanation.

On the other hand, in the case of IS collisions (e.g., with $x_1 = -31$ and $x_2 = 30$), we expect a significant change in the phenomenology, as in this case the collision point is at a local maximum of the PN potential, while in the OS case it was at a local minimum. This important difference results in a strong reduction of the scale of the initial velocity (determining the different outcomes of the IS collisions), roughly by an order of magnitude, as compared to the OS case. Apart this reduction, most features of the phenomenology discussed above for the OS collisions can also be found in the case of IS collisions. Nevertheless, in the case of IS collisions with the intermediate value of the amplitude $B = 1$, and for $0.062 < a < 0.075$, lead to spontaneous SB, with mutual reflection (rather than merger) of the solitons after multiple collisions, see left panel of Fig. 17.4 (note that the collision results in a merger for $a < 0.061$ and $0.075 < a < 0.089$, while it is quasi-elastic for $a > 0.089$). Such a *multiple-bounce* window in the DNLS system, resembles a similar effect that was found for ϕ^4 kinks in [17, 18], but with an important difference that in the kink-bearing models, spontaneous SB is impossible. Finally, it should be mentioned that quarter-site collisions (corresponding, e.g., to $x_1 = -29.5$ and

$x_2 = 30$) lead also to qualitatively similar results: for the smaller amplitude value of $B = 0.851$ the collision results in the separation of solitons upon a single bounce with SB for all values of a, while for the larger amplitude value of $B = 1.175$ there exist windows of no collision (for $0 < a < 0.5$), formation of a static bound state, in the form of "M" (for $0.5 < a < 0.9$, see right panel of Fig. 17.4) and quasi-elastic collision with SB (for $a > 0.9$).

17.4 Strongly Discrete Nearly Integrable Case

Here, following [7], we discuss the weakly perturbed integrable AL system Eq. (17.2), in the regime of high discreteness setting $C = 0.78$ and small values for the perturbation parameters, δ and ε. In the simulations, initial conditions were set according to the exact AL soliton solution in Eq. (17.3).

In Fig. 17.5 the soliton amplitudes after collision, $\tilde{A}_i$, are shown as functions of the initial phase difference $\Delta\alpha_0$ for different coordinates of the collision point, x_c, with respect to the lattice: (a) $x_c = 0$ (OS collision), (b) $x_c = 0.25$, (c) $x_c = 0.5$ (IS collision), and (d) $x_c = 0.75$. It is readily seen that the collisions are inelastic only in the vicinity of $\Delta\alpha_0 = 0$, the situation typical for the weakly perturbed integrable systems. However, in contrast to the result presented in Fig. 17.1d for the weak discreteness, in the highly discrete case, as it was already described in Sect. 17.3, the collision outcome becomes extremely sensitive to the location of the collision point with respect to the lattice. For example, collisions of in-phase solitons ($\Delta\alpha_0 = 0$) are practically elastic for $x_c = 0$ and $x_c = 0.5$, while they are strongly inelastic

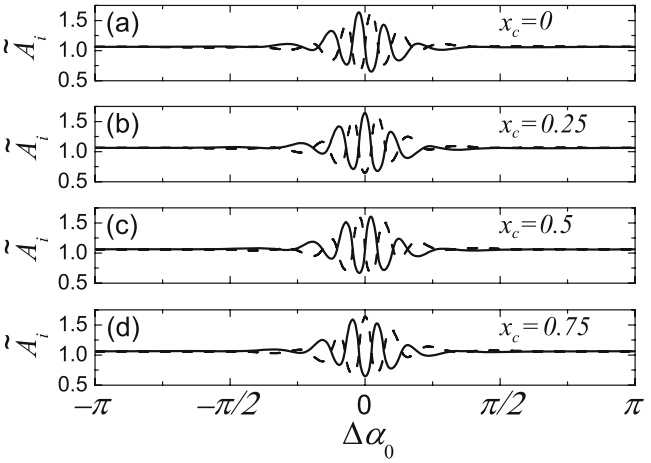

Fig. 17.5 Soliton amplitudes after collision, $\tilde{A}_i$, as the functions of the initial phase difference $\Delta\alpha_0$ for different coordinates of the collision point x_c with respect to the lattice: (**a**) $x_c = 0$ (on-site collision), (**b**) $x_c = 0.25$, (**c**) $x_c = 0.5$ (inter-site collision), and (**d**) $x_c = 0.75$. The soliton parameters before the collision are $\mu_1 = \mu_2 = 0.75$, $k_1 = -k_2 = 0.1$. The model parameters are $\delta = 0.04$, $\varepsilon = 0$, and $C = 0.78$

for $x_c = 0.25$ and $x_c = 0.75$. For any x_c, in the vicinity of $\Delta\alpha_0 = 0$, the collision outcome is extremely sensitive to small variations in $\Delta\alpha_0$, which is typical for the near-separatrix collisions.

We emphasize again that in the weakly perturbed integrable system, also in the case of strong discreteness, the dominant inelasticity effect is the REE between colliding solitons, while the radiation losses and the excitation of the soliton's internal modes are marginal even for the near-separatrix collisions with $\Delta\alpha_0 \approx 0$ [7].

The model Eq. (17.2) contains the perturbation parameters δ and ϵ (determining the strength of the cubic and quintic perturbation terms, respectively). In Fig. 17.6 we show the maximal degree of inelasticity of the collision as a function of δ at $\varepsilon = 0$ (a) and ε at $\delta = 0$ (b). The ordinate is the maximal (over x_c and $\Delta\alpha_0$) soliton amplitude after collision, $\tilde{A}_{\max}$. The discreteness parameter is $C = 0.78$. The soliton velocities and amplitudes before the collision are $V_1 = -V_2 = 0.137$ and $A_1 = A_2 = 1.05$, respectively.

The results presented in Fig. 17.6 reveal the asymmetry in the net inelasticity effect for positive and negative values of the perturbation parameters δ and ε. In (a) the asymmetry appears for $|\delta| > 0.02$ and in (b) for $|\varepsilon| > 0.0025$ and it is negligible for smaller values of perturbation parameters. This asymmetry can be explained through the influence of the soliton's internal modes that exist, as it is well-known, only if the perturbation parameter has the "right" sign [19]. To confirm this, we calculate the spectrum of small amplitude vibrations of the lattice containing a stationary soliton with frequency $\omega = 2C(\cosh\mu - 1)$ (for the chosen parameters $\omega = 0.4$). The spectrum includes the phonon band $\Omega = \pm[4C\sin^2(Q/\sqrt{8C}) + \omega]$, where Q and Ω are the phonon wave number and frequency, respectively, and it may include the frequencies of soliton's internal modes. The results are presented in Fig. 17.7. In (a) and (b) we show the bifurcation of the internal mode frequency, $\omega_{\rm IM}$, from the upper edge of the phonon spectrum, $\Omega_{\max}$, while in (c) and (d) from the lower edge of the spectrum, $\Omega_{\min}$. Particularly, we plot $\sqrt{\omega_{\rm IM} - \Omega_{\max}}$ as a function of δ at $\varepsilon = 0$ (a), and ε at $\delta = 0$ (b), and also we plot $\sqrt{\Omega_{\min} - \omega_{\rm IM}}$ as a function of δ at $\varepsilon = 0$ (c) and ε at $\delta = 0$ (d). Recall that $C = 0.78$.

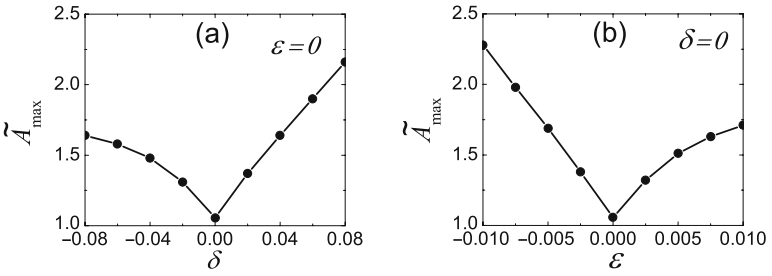

Fig. 17.6 Maximal (over x_c and $\Delta\alpha_0$) soliton amplitude after collision as a function of (**a**) δ at $\varepsilon = 0$ and (**b**) ε at $\delta = 0$. The discreteness parameter is $C = 0.78$. The soliton velocities before the collision are $V_1 = -V_2 = 0.137$ and the amplitudes before the collision are $A_1 = A_2 = 1.05$

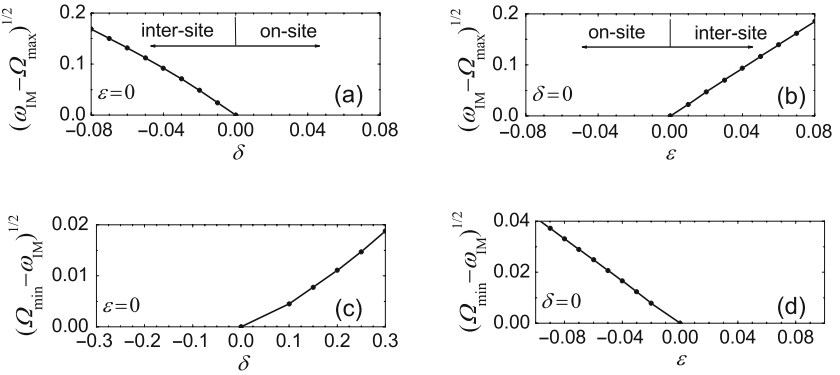

Fig. 17.7 Bifurcation of the soliton's internal mode frequency $\omega_{\rm IM}$ from (**a, b**) the upper edge of the phonon spectrum, $\Omega_{\rm max}$, and (**c, d**) from the lower edge of the phonon spectrum, $\Omega_{\rm min}$. In (**a, c**) $\varepsilon = 0$, while in (**b, d**) $\delta = 0$. In all cases the stationary soliton has frequency $\omega = 0.4$ and the discreteness parameter is $C = 0.78$

The numerical results show that the solitons emerge from the collision bearing internal modes with frequencies corresponding to the lower edge of the spectrum and, thus, it can be concluded that these modes can influence the collision outcome but not the modes bifurcating from the upper edge.

Coming back to the asymmetry of the inelasticity of collisions with respect to the change of the sign of perturbation parameter (see Fig. 17.6), it can now be concluded that the net inelasticity effect is higher when the soliton's internal modes come into play. More precisely, at $\varepsilon = 0$ the collisions are more inelastic for $\delta > 0$ when the internal mode below the phonon band exists. Similarly, for $\delta = 0$ collisions are more inelastic for $\varepsilon < 0$, for the same reason.

We note in passing that a change of the sign of perturbation parameters switches the stable OS and IS configurations as indicated in Fig. 17.7a, b.

17.5 Role of Soliton's Internal Modes

As mentioned above, the REE is the dominant effect in soliton collisions in the weakly perturbed NLS or AL systems. However, if the perturbation is not small, the REE effect is mixed with radiation and possibly with excitation of the soliton's internal modes. In Sect. 17.4 we have already discussed the role of the soliton's internal modes and here we further elaborate on their role in the inelastic soliton collisions.

Particularly, we will now investigate if the energy exchange between the soliton's internal and translational modes is possible in the perturbed NLS equation. Such energy exchange plays an important role in the collisions among ϕ^4 kinks resulting in several nontrivial effects such as separation after multiple-bounce collisions [17, 18, 20–23]. In order to eliminate the influence of the location of the collision

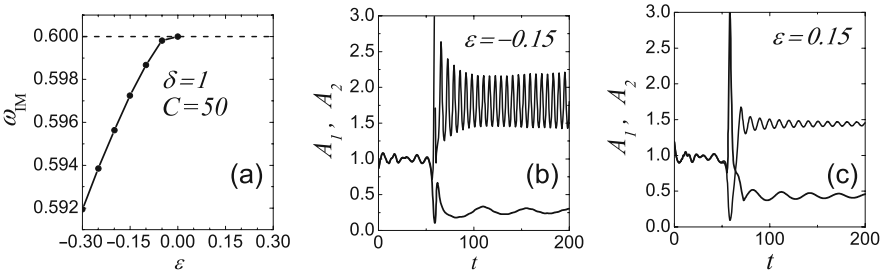

Fig. 17.8 (**a**) Bifurcation of the soliton's internal mode frequency $\omega_{\rm IM}$ from the lower edge of the phonon spectrum as the function of perturbation parameter ε at $\delta = 1$, $C = 50$ for the stationary soliton with frequency $\omega = 0.6$. An internal mode exists only for $\varepsilon < 0$. Panels (**b**) and (**c**) show the amplitudes of solitons as a function of time for moderately perturbed systems with $\varepsilon = -0.15$ and 0.15, respectively. Solitons having initial amplitudes $A_1 = A_2 \approx 1$ and velocities $V_1 = -V_2 = 0.05$ collide at $t \approx 60$ and they emerge from the collision with different amplitudes. Moreover, in (b), high-amplitude internal modes with very long lifetime are excited, while in (c), they are not. Initial phase difference in both cases is $\Delta\alpha_0 = 0.12$

point with respect to the lattice we set in Eq. (17.2) $C = 50$ (extremely weak discreteness) and take $\delta = 1$, so that the cubic perturbation is absent and the only perturbation remains to be the quintic term with coefficient ε.

In Fig. 17.8a we show the bifurcation of the soliton's internal mode frequency $\omega_{\rm IM}$ from the lower edge of the phonon spectrum $\Omega_{\rm min} = \omega$ (where $\omega = 0.6$ is the soliton's frequency) as a function of ε. The internal mode exists only for $\varepsilon < 0$. The panels (b) and (c) of the same figure show the amplitudes of the solitons as a function of time for $\varepsilon = -0.15$ and 0.15, respectively. Solitons having initial amplitudes $A_1 = A_2 \approx 1$ and velocities $V_1 = -V_2 = 0.05$ collide at $t \approx 60$. The initial phase difference is $\Delta\alpha_0 = 0.12$.

Figure 17.8 clearly illustrates that in the case of $\varepsilon < 0$, when the internal mode exists, the collision is more inelastic than in the case of $\varepsilon > 0$. In addition to this, in the case of $\varepsilon < 0$ the solitons emerge from the collision bearing high-amplitude internal modes with very long lifetime, while in (c) such modes are not excited.

Now we focus on the case of $\varepsilon = -0.15$ and study the symmetric in-phase solitons ($\Delta\alpha_0 = 0$) with different velocity V for solitons with initial amplitudes $A_1 = A_2 = 1$. Relevant results are shown in Fig. 17.9. In (a) we plot the velocity of the solitons after collision, $\tilde{V}$, as a function of V. For the collision velocity $V > V^* \approx 0.42$, the solitons separate after the collision while for $V < V^*$ they merge. An example of collision with merger for the collision velocity $V = 0.4$ is given in (c) where only the particles with $|u_n|^2 > 0.2$ are shown. No separation "windows" in the region $V < V^*$, typical for the kink collisions in ϕ^4 model, are found. In (b), for the velocities $V < V^*$ we plot the maximal separation $S_{\rm max}$ of two solitons after the first collision as a function of V. If the energy exchange between the soliton's internal and translational modes took place, one would see the maxima of $S_{\rm max}$ at the resonant collision velocities, but nothing like that is observed. It should be pointed out that the high-amplitude internal modes *are* excited during the collision, similar

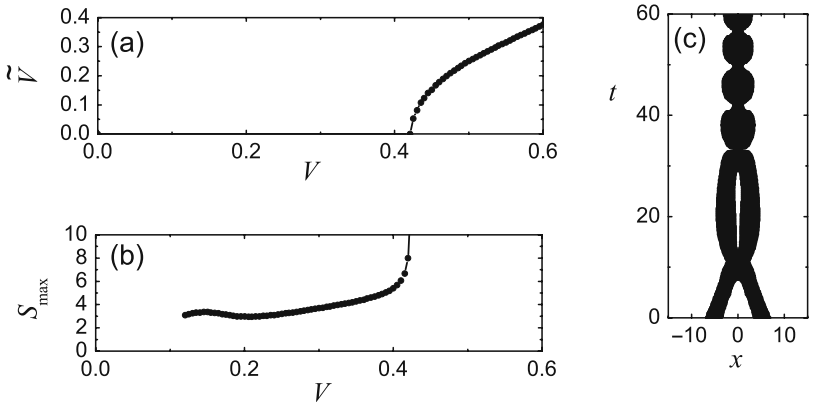

Fig. 17.9 Role of internal modes studied by colliding the symmetric in-phase solitons ($\Delta\alpha_0 = 0$) with velocity V in the moderately perturbed NLS equation Eq. (17.2) with $C = 50$ (extremely weak discreteness), $\varepsilon = -0.15$, $\delta = 1$. The initial soliton amplitudes are $A_1 = A_2 = 1$. (**a**) The velocity of solitons after collision, $\tilde{V}$, is shown as a function of V. (**b**) The maximal separation $S_{\max}$ of two solitons after the first collision is given as a function of V. (**c**) Example of collision for the collision velocity $V = 0.4$. Shown are the particles with $|u_n|^2 > 0.2$

to that shown in Fig. 17.8b but, in contrast to the ϕ^4 case, they do not significantly affect the translational motion of the solitons.

Another important note is the following: in the simulations presented in Fig. 17.9 we have excluded the REE effect by setting $\Delta\alpha_0 = 0$. For nonzero $\Delta\alpha_0$, in the vicinity of $\Delta\alpha_0 = 0$, the REE effect would completely change the collision outcome, and particularly, the soliton separation after multi-bounce collisions could be observed.

17.6 Solitary Wave Collisions in Physically Relevant Settings

In this section, we will discuss some physically relevant settings where solitary wave collisions in weakly discrete or discrete systems have been investigated. These include optical waveguide arrays in the nonlinear optics context, and BECs confined in periodic potentials, so-called optical lattices, in the atomic physics context.

First, in the context of nonlinear optics, in [24] (see also related work in [25]), the interaction of two solitary waves was studied experimentally in arrays of AlGaAs coupled optical waveguides. In this case, the relevant mathematical model is the discrete cubic NLS equation discussed above. The focus in this experimental work was on the case of the interaction of solitons with zero initial velocities (in terms of the nomenclature of the present work), and a result coinciding with our findings was that, in the limit of the zero collision velocity, two solitons with the zero phase difference always merge into one.

Soliton mobility [26] and collisions [27–29] were studied theoretically in the framework of a discrete NLS equation with a saturable nonlinearity. In particular, the nonlinear term in the DNLS equation was taken to be of the form

$-\beta u_n/(1 + I_n)$, (here $I_n \sim |u_n|^2$ is the normalized light peak intensity and $\beta =$ const.). This type of the discrete NLS equation is also called Vinetskii–Kukhtarev model (VK) [30], which is particularly relevant to waveguide arrays created in photorefractive crystals. The latter have attracted much attention (see, e.g., the reviews [31, 32]) as they offer real-time control of the waveguide array, as well as strong and tunable nonlinearity [33]. Note that for low-norm solutions the VK model is reduced to the cubic discrete NLS equation.

In [27] it was found that, similarly to the results of Sect. 17.2, low-norm solitons with small velocities merge and remain pinned, creating a breathing state, while for high enough velocities, the solitons are reflected. However, high-norm moving solutions are also allowed in the VK model [26, 29] (contrary to the cubic DNLS case, due to the potential vanishing of the PN barrier relevant to the VK case). When high-norm (power) solutions collide the effect of, so-called, breather creation can be observed [27, 29], consisting of a partial trapping of the energy of the incoming solitons, together with the reflection of the initial solitons. Note that this effect was previously found in the continuum counterpart of the model [34].

Symmetric collisions of two discrete breathers in the VK model were also investigated in [28]. The strong correlation of the collision properties and the parameters of colliding breathers (power, velocity, and phase difference), lattice parameters and position of the collision point was related to the internal structure of the colliding breathers and energy exchange with the phonon background. Several types of collision were observed in wide parameter space: elastic (quasi-elastic) OS (IS) collision, breather creation, fusion of colliding breathers, and creation of two asymmetric breathers (after IS collision).

Soliton collisions were also studied in the context of BECs trapped in a periodic potential created by the interference of optical beams, the so-called optical lattice [35]. In this case, the pertinent model describing the evolution of the BEC wave function is the continuous NLS (with a periodic external potential) equation or the discrete NLS equation, for a weak or strong (as compared to the system's chemical potential) optical lattice strength, respectively [36]. In the former case, collisions of the pertinent, so-called lattice solitons have been studied in various works (see, e.g., [37, 38]), while the transition from the continuous to discrete regime was studied in [39]. In this work, the outcome of the collision between two gap solitons was shown to serve as a measure of the discreteness imposed on the BEC by the optical lattice. Moreover, in [40], soliton collisions were studied in the framework of a strongly discrete NLS equation with a periodically time-modulated nonlinearity coefficient. This model describes a BEC confined in a strong optical lattice, whose interatomic interactions (effectively described by the nonlinear term in the NLS model) are controlled by time-periodic external fields, according to the so-called Feshbach resonance management technique [41]. Such a time-dependent variation of the nonlinearity was shown to assist the discrete soliton motion, and a study of soliton collisions revealed that there exist two different types of the interaction: elastic bounce, or bounce with mass transfer from one soliton to the other. It is relevant to note that, in contrast to the results of Sect. 17.3 (where the DNLS equation had constant coefficients), in the model analyzed in [40] a merger of colliding solitons into a standing one was not observed.

17.7 Conclusions

The above discussion of the effects observed in solitary wave collisions in 1D DNLS equation in the regimes of weak and strong discreteness for nearly integrable and nonintegrable cases can be summarized as follows.

For *nearly integrable systems*, i.e., for the integrable NLS equation perturbed by weak discreteness and for the weakly perturbed AL chain at any degree of discreteness, the inelasticity of collisions is solely due to the radiationless energy exchange between solitons with relatively small amount of radiation and almost no excitation of the soliton's internal modes. This is so because the radiationless energy exchange grows proportionally to the perturbation parameter [5, 11] while the radiation and excitation of the internal modes are the second-order effects [19].

The radiationless energy exchange happens in the vicinity of multisoliton separatrix solutions to the corresponding integrable equations [5]. Typical features of near-separatrix collisions in nearly integrable systems are as follows:

- Collisions are inelastic in a narrow window of parameters of colliding solitons while outside this window they are practically elastic. Examples are presented in Fig. 17.1d for the weakly discrete NLS equation and in Fig. 17.5 for the weakly perturbed AL lattice at high discreteness. Collisions are inelastic only for nearly in-phase (near separatrix) collisions with $\Delta\alpha_0 \sim 0$ [5].
- Near-separatrix collisions are naturally extremely sensitive to small variations in the collision phase $\Delta\alpha_0$ and, for highly discrete systems, to the location of the collision point with respect to the lattice (see Figs. 17.1d and 17.5).
- The fact that the inelasticity of soliton collisions for weakly perturbed systems increases linearly with the perturbation parameter is illustrated by Fig. 17.6. Panel (a) suggests that in the case $\varepsilon = 0$, the radiationless energy exchange effect is dominant within $|\delta| < 0.02$, while from panel (b), for $\delta = 0$, it is dominant for $|\varepsilon| < 0.0025$. For larger values of perturbation parameters, the soliton's internal modes start to affect the result of collision and the net inelasticity effect becomes asymmetric for positive and negative values of perturbation parameters.
- The radiationless energy exchange effect in near-separatrix collisions has been predicted from the analysis of the two-soliton solution to the *unperturbed* integrable NLS equation [5] and thus the actual type of perturbation is not important for the appearance of this effect. It has been also demonstrated that in the systems with more than one perturbation term, the collisions can be nearly elastic even in the vicinity of $\Delta\alpha_0 = 0$ when the effects of different perturbations cancel each other [5, 7].
- The inelasticity of collision increases with decrease in collision velocity. This feature is again related to the near-separatrix nature of the collision. Fast solitons spend a shorter time in the vicinity of separatrix during the collision and their properties are less affected than that of slow solitons.
- The radiationless energy exchange can be responsible for the fractal soliton scattering [4] if they collide with sufficiently small velocities, which is illustrated by the results presented in Fig. 17.2.

– The radiationless energy exchange effect is possible only if the number of parameters of the colliding solitons exceeds the number of conservation laws in the weakly perturbed system [42]. For example, in the weakly discrete Frenkel–Kontorova model, the conservation of energy (exact) and momentum (approximate) sets two constraints on the soliton parameters and, as a result, the two-kink collisions are practically elastic. A three-kink collision has one free parameter and radiationless energy exchange becomes possible [43]. Solitons in the NLS equation and AL chain have two parameters so that the two-soliton collisions are described by four parameters. If in the weakly perturbed NLS equation or AL lattice, the number of exact and approximate conservation laws is less than four (typically this is so) then the radiationless energy exchange is possible in two-soliton collisions.
– In the *moderately or strongly perturbed* systems the soliton collisions become even more complicated because in addition to the radiationless energy exchange the excitation of the soliton's internal modes and radiation become important and the net inelasticity effect is an admixture of these three effects.

  Particularly, for the strongly discrete, nonintegrable case, the merger of colliding solitons can be observed in certain range of collision velocities (see the results shown in Figs. 17.3 and 17.4). Another interesting effect of strong nonintegrability is the symmetry breaking effect described in Sect. 17.3. In the case of high discreteness, the collision outcome in a nonintegrable system is extremely sensitive to location of the collision point with respect to the lattice.
– When the soliton internal modes come into play, the radiationless energy exchange effect becomes more pronounced (compare panels (b) and (c) of Fig. 17.8). The soliton internal modes result in the asymmetry of the net inelasticity effect with respect to the change of sign of perturbation parameter, see Fig. 17.6. In Sect. 17.5 we have analyzed the influence of high-amplitude soliton's internal modes on the collision outcome for the NLS equation with moderate quintic perturbation in the absence of the radiationless energy exchange effect. We found that, in spite of the fact that the high-amplitude internal modes *are* excited during the collision, they do not significantly affect the translational motion of the solitons. This behavior contrasts that observed for the colliding ϕ^4 kinks
  [17, 18, 20–23].

17.8 Future Challenges

Before closing, we would like to mention various interesting open problems that, in our opinion, deserve to be studied in more detail.

(i) In many physically relevant cases, 2D and 3D models describe realistic situations better than 1D models, but the solitary wave collisions in higher dimensions have been studied much less than in the 1D case.

(ii) Collisions between discrete vector solitons have not been studied in detail. In fact, although this issue was studied theoretically for waveguide arrays with the Kerr-type nonlinearity [44] (relevant experiments were reported in [45]), the case of vector soliton collisions in coupled discrete Vinetskii-Kukhtarev models has not been considered so far. This is an interesting direction, since relevant experimental [2] and theoretical [46] results have already appeared recently. Moreover, as per our previous remark, discrete vector soliton collisions in higher dimensional settings have not been studied in detail yet. Such studies would be particularly relevant in the context of multicomponent and spinor BECs [36].

(iii) The interplay between various mechanisms controlling the inelasticity of soliton collisions (e.g., radiationless energy exchange, internal modes, and radiation) is not fully understood yet even in 1D settings.

(iv) For nearly integrable models, the collision outcome depends on the number of exact and approximate conservation laws remaining in the system. However, so far, a detailed study on how a perturbation affects the conservation laws of an integrable equation is still missing.

(v) Some results presented here are not fully understood and certainly deserve a more careful consideration. For example, as concerns the findings of Sect. 17.5, it is worth noting the following. Contrary to what is observed in kink collisions in the ϕ^4 model, soliton collisions in continuum NLS equation with quintic perturbation do not reveal a noticeable interaction between the soliton's translational and internal modes. This observation should be better understood and explained.

Acknowledgments It is a pleasure and an honor to acknowledge the invaluable contribution of our colleagues and friends with whom we had a very pleasant and productive collaboration on this interesting and exciting topic: P. G. Kevrekidis, Yu. S. Kivshar, B. A. Malomed, A. E. Miroshnichenko, I. E. Papacharalampous, D. A. Semagin, T. Shigenari, A. A. Sukhorukov, and A. A. Vasiliev are greatly thanked.

References

1. Kivshar, Yu.S., Agrawal, G.P.: Optical Solitons: From Fibers to Photonic Crystals. Academic Press, San Diego (2003) 311
2. Ablowitz, M.J., Ladik, J.F.: J. Math. Phys. **16**, 598 (1975) 311, 312
3. Ablowitz, M.J., Ladik, J.F.: J. Math. Phys. **17**, 1011 (1976) 311, 312
4. Dmitriev, S.V., Shigenari, T.: Chaos **12**, 324 (2002) 311, 313, 314, 324
5. Dmitriev, S.V., Semagin, D.A., Sukhorukov, A.A., Shigenari, T.: Phys. Rev. E **66**, 046609 (2002) 311, 312, 313, 314, 315, 324
6. Papacharalampous, I.E., Kevrekidis, P.G., Malomed, B.A., Frantzeskakis, D.J.: Phys. Rev. E **68**, 046604 (2003) 311, 315, 316, 317
7. Dmitriev, S.V., Kevrekidis, P.G., Malomed, B.A., Frantzeskakis, D.J.: Phys. Rev. E **68**, 056603 (2003) 311, 312, 315, 318, 319, 324
8. Salerno, M.: Phys. Rev. A **46**, 6856 (1992) 312
9. Sukhorukov, A.A., Akhmediev, N.N.: Phys. Rev. Lett. **83**, 4736 (1999) 312

10. Gordon, J.P.: Opt. Lett. **8**, 596 (1983) 312
11. Frauenkron, H., Kivshar, v, Malomed, B.A.: Phys. Rev. E **54**, R2244 (1996) 313, 324
12. Zhu, Y., Yang, J.: Phys. Rev. E **75**, 036605 (2007) 313
13. Zhu, Y., Haberman, R., Yang, J.: Phys. Rev. Lett. **100**, 143901 (2008) 313
14. Karpman, V.I., Solov'ev, V.V.: Physica D **3**, 142 (1981) 313
15. Malomed, B.A., Weinstein, M.I.: Phys. Lett. A **220**, 91 (1996) 315
16. Kaup, D.J.: Math. Comput. Simul. **69**, 322 (2005) 315
17. Campbell, D.K., Schonfeld, J.F., Wingate, C.A.: Physica D **9**, 1 (1983) 317, 320, 325
18. Campbell, D.K., Peyrard, M.: Physica D **18**, 47 (1986) 317, 320, 325
19. Kivshar, Yu.S., Pelinovsky, D.E., Cretegny, T., Peyrard, M.: Phys. Rev. Lett. **80**, 5032 (1998) 319, 324
20. Anninos, P., Oliveira, S., Matzner, R.A.: Phys. Rev. D **44**, 1147 (1991) 320, 325
21. Belova, T.I., Kudryavtsev, A.E.: Phys. Usp. **40**, 359 (1997) 320, 325
22. Goodman, R.H., Haberman, R.: SIAM J. Appl. Dyn. Sys. **4**, 1195 (2005) 320, 325
23. Goodman, R.H., Haberman, R.: Phys. Rev. Lett. **98**, 104103 (2007) 320, 325
24. Meier, J., Stegeman, G.I., Silberberg, Y., Morandotti, R., Aitchison, J.S.: Phys. Rev. Lett. **93**, 093903 (2004) 322
25. Meier, J., Stegeman, G., Christodoulides, D., Morandotti, R., Sorel, M., Yang, H., Salamo, G., Aitchison, J., Silberberg, Y.: Opt. Express **13**, 1797 (2005) 322
26. Melvin, T.R.O., Champneys, A.R., Kevrekidis, P.G., Cuevas, J.: Phys. Rev. Lett. **97**, 124101 (2006) 322, 323
27. Cuevas, J., Eilbeck, J.C.: Phys. Lett. A **358**, 15 (2006) 322, 323
28. Maluckov, A., Hadžievski, Lj., Stepić, M.: Eur. Phys. J. B **53**, 333 (2006) 322, 323
29. Melvin, T.R.O., Champneys, A.R., Kevrekidis, P.G., Cuevas, J.: Physica D **237**, 551 (2008) 322, 323
30. Vinetskii, V.O., Kukhtarev, N.V.: Sov. Phys. Solid State **16**, 2414 (1975) 323
31. Fleischer, J.W., Bartal, G., Cohen, O., Schwartz, T., Manela, O., Freedman, B., Segev, M., Buljan, H., Efremidis, N.K.: Opt. Express **13**, 1780 (2005) 323
32. Chen, Z., Martin, H., Eugenieva, E.D., Xu, J., Yang, J.: Opt. Express **13**, 1816 (2005) 323
33. Efremidis, N.K., Sears, S., Christodoulides, D.N., Fleischer, J.W., Segev, M.: Phys. Rev. E **66**, 046602 (2002) 323
34. Królikowski, W., Luther-Davies, B., Denz, C.: IEEE J. Quantum Electron. **39**, 3 (2003) 323
35. Morsch, O., Oberthaler, M.K.: Rev. Mod. Phys. **78**, 179 (2006) 323
36. Kevrekidis, P.G., Frantzeskakis, D.J., Carretero-González, R. (eds.): Emergent Nonlinear Phenomena in Bose-Einstein Condensates: Theory and Experiment. Springer Series on Atomic, Optical, and Plasma Physics, vol. 45 2007 323, 326
37. Sakaguchi, H., Malomed, B.A.: J. Phys. B: At. Mol. Opt. Phys. **37**, 1443 (2004) 323
38. Ahufinger, V., Sanpera, A.: Phys. Rev. Lett. **94**, 130403 (2005) 323
39. Dąbrowska, B.J., Ostrovskaya, E.A., Kivshar, Yu.S.: J. Opt. B: Quantum Semiclass. Opt. **6**, 423 (2004) 323
40. Cuevas, J., Malomed, B.A., Kevrekidis, P.G.: Phys. Rev. E **71**, 066614 (2005) 323
41. Kevrekidis, P.G., Theocharis, G., Frantzeskakis, D.J., Malomed, B.A.: Phys. Rev. Lett. **90**, 230401 (2003) 323
42. Kevrekidis, P.G., Dmitriev, S.V.: Soliton collisions. In: Scott, A. (ed.) Encyclopedia of Nonlinear Science, pp. 148–150. Routledge, New York (2005) 325
43. Miroshnichenko, A.E., Dmitriev, S.V., Vasiliev, A.A., Shigenari, T.: Nonlinearity **13**, 837 (2000) 325
44. Ablowitz, M.J., Musslimani, Z.H.: Phys. Rev. **65** 056618 (2002) 326
45. Meier, J., Hudock, J., Christodoulides, D.N., Stegeman, G., Silberberg, Y., Morandotti, R., Aitchison, J.S.: Phys. Rev. Lett. **91**, 143907 (2003) 326
46. Fitrakis, E.P., Kevrekidis, P.G., Malomed, B.A., Frantzeskakis, D.J.: Phys. Rev. E **74**, 026605 (2006) 326